Interference Avoidance in Spectrally Encoded Multiple Access Communications Using MPSK Modulation

A.S. Nunez, M.A. Temple, R.F. Mills and R.A. Raines
Department of Electrical and Computer Engineering
Air Force Institute of Technology
Wright-Patterson AFB, OH 45433

***Abstract*— Spectral encoding is employed to provide interference avoidance and multiple access capability using M-ary phase shift keyed (MPSK) data modulation. Communication symbols are formed using composite phase modulation (independent data and coded multiple access) on selected spectral components and then inverse Fourier transforming to obtain time domain waveforms. This technique enables multiple access and adaptive channel interference suppression. One inherent advantage is analytic tractability of phase modulation components across domains which enables robust theoretical performance prediction with variation in multiple access phase value assignment. Detection and estimation is accomplished using conventional correlation receiver techniques and error performance is shown to be consistent with conventional MPSK signaling. Analytic and simulated results are provided for multiple access bit error performance and interference suppression demonstrated using randomly assigned, uniformly distributed multiple access phase values.**

I. Introduction

Spectrally encoded communication techniques have been shown capable of providing considerable protection from various types of interference while providing effective multiple access capability [1, 2]. Such techniques have generally employed M-ary cyclic shift keying, a form of orthogonal signaling, as the primary data modulation. Expanding upon previous work, a form of spectrally encoded M-ary Phase Shift Keying (MPSK) is introduced whereby phase modulation (independent data and coded multiple access) is applied in the frequency domain, and demodulation is performed in the time domain [3]. In conjunction with providing effective multiple access communications with interference avoidance mechanisms, the proposed technique is attractive because the phase modulation factors are analytically tractable between frequency and time domains. This tractability permits detailed development, analysis and characterization of communication performance. Analytic development of frequency and time domain representations of spectrally encoded MPSK signals is provided, and multiple access communication performance (bit error rate) validated via simulation. Spectrally encoded MPSK performance is shown to be consistent with conventional MPSK signaling while providing interference avoidance (suppression) commensurate with that of previous orthogonal transform domain techniques.

II. Spectrally Encoded MPSK Symbol Development

Spectrally encoded MPSK signaling begins in the frequency domain where composite phase modulation, comprised of independent data and coded multiple access components, are applied to sinusoidal components. Although this spectral modulation process is conceptually similar to orthogonal frequency division multiplexing (OFDM) [4], the modulation process here differs in that the data phase modulation is *constant* across all spectral components. The m^{th} spectrally encoded MPSK communication symbol for user v is generated from

$$S_m^{(v)}(f) = \sum_{k=1}^{K} A_k^{(v)} \left[\Delta_k^- + \Delta_k^+\right] \tag{1}$$

$$\Delta_k^- = \delta(f - kf_{sb}) e^{+j\left[\phi_k^{(v)} + \theta_m^{(v)}\right]} \tag{2}$$

$$\Delta_k^+ = \delta(f + kf_{sb}) e^{-j\left[\phi_k^{(v)} + \theta_m^{(v)}\right]} \tag{3}$$

where superscript v in (1) denotes a specific user, $v \in [1, 2, ..., N_u]$, subscript m denotes a specific communication symbol, $m \in [1, 2, ..., M]$, K is the number of sinusoidal components, f_{sb} is sinusoidal component spacing (symbol frequency), $T_{sb} = 1/f_{sb}$ is symbol duration, A_k is the amplitude weight of the k^{th} component, $A_k \geq 0$, $\theta_m^{(v)}$ is the *Data Phase Modulation* for the m^{th} symbol of user v, and $\phi_k^{(v)}$ is the *Coded Multiple Access (MA) Phase Modulation* for user v.

The time domain representation of spectrally encoded MPSK symbols is obtained by taking the inverse Fourier transform of (1), yielding symbols of the form [3]

$$s_m^{(v)}(t) = 2\sum_{k=1}^{K} A_k^{(v)} \cos\left[2\pi f_{sb} kt + \phi_k^{(v)} + \theta_m^{(v)}\right] \tag{4}$$

for $0 \leq t \leq T_{sb}$ and having total symbol energy over interval T_{sb} equaling

$$E_{s_m^{(v)}} = 2T_{sb} \sum_{k=1}^{K} \left[A_k^{(v)}\right]^2 \quad \forall\, m \in [1, 2, ..., M] \tag{5}$$

It was noted earlier that sinusoidal amplitudes are assigned such that $A_k \geq 0$. The inclusion of zero amplitude values is specifically permitted such that 1) it is possible to avoid transmitting energy in selected spectral regions such that interference with other systems may be intentionally avoided, or 2) the transmitted communication signals of interest "avoid" crowded spectral regions and interference effects are minimized during receiver detection and estimation, i.e., the receiver avoids extracting energy (noise and other interfering signals) from spectral regions where no signal energy was intentionally placed; this is the fundamental spectral notching and interference avoidance mechanism demonstrated previously in transform domain communication systems [1, 2]. In the interference avoidance case where symbols are specifically designed to avoid spectrally crowded regions, symbol energy is generally scaled following spectral notching to ensure all communication symbols are transmitted with equal energy (assuming of course that equal energy signaling is the goal).

Communication performance using the spectrally encoded waveform of (4) is characterized by considering the cross correlation between two communication symbols for user v. Considering the m^{th} and n^{th} communication symbols of (4), and the symbol energy expression of (5), integration over symbol interval T_{sb} yields symbol cross correlation $R_{mn}^{(v)}$ given by

$$R_{mn}^{(v)} = E_s^{(v)} \cos\left[\theta_m^{(v)} - \theta_n^{(v)}\right] \tag{6}$$

assuming equal energy signaling such that $E_{s^{(v)}} = E_{s_m^{(v)}} = E_{s_n^{(v)}}$ for all m and n. Cross correlation results of (6) clearly indicate how symbol phase value assignment dictates communication performance.

A. Communication Performance

Using data phase modulation of $\theta_m = (2\pi m/M)$ for $M = 2^l$ communication symbols, produces $R_{mn}^{(v)}$ characteristics similar to conventional MPSK signaling such that (6) dictates correlation receiver performance. Thus, the spectrally encoded MPSK technique achieves theoretic bit error probability (P_b) equivalent to conventional MPSK. An analytic P_b expression for binary phase shift keying, using optimum coherent detection over an AWGN channel, is given by (7) where E_b is average energy per bit and N_o is noise power spectral density. For $M > 2$ and large energy to noise ratios, P_b is well approximated by (8) assuming Gray code bit-to-symbol mapping [5].

$$P_b = Q\left[\sqrt{2\left(\frac{E_b}{N_o}\right)}\right] \tag{7}$$

$$P_b \approx \frac{2Q}{l}\left[\sqrt{2l\left(\frac{E_b}{N_o}\right)}\sin\left(\frac{\pi}{M}\right)\right] \tag{8}$$

Communication results from Monte Carlo simulation of $M = 2,\ 4,\ 8$ and 16 spectrally encoded MPSK signaling are shown in Fig. 1 for $K = 255$ sinusoidal components. Note that

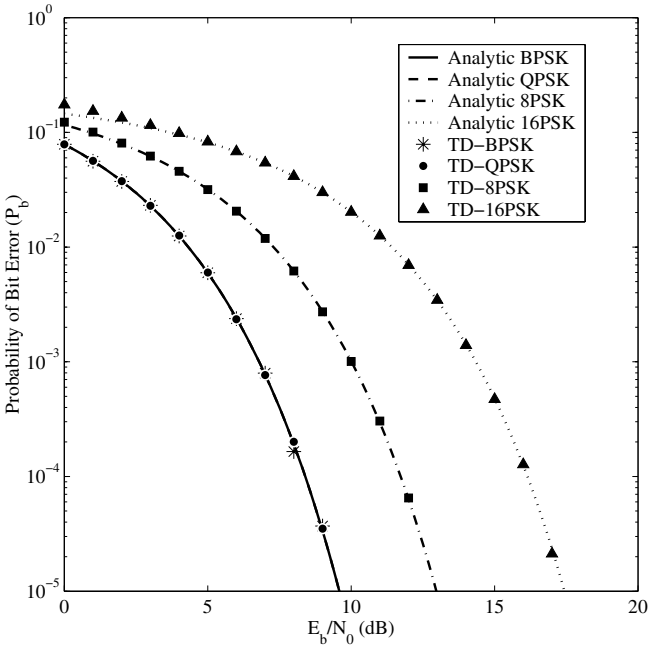

Fig. 1. Communication Performance: P_b versus E_b/N_o for Spectrally Encoded MPSK Using $K = 255$ Sinusoidal Components [3]

the $M = 2$ and $M = 4$ data is virtually coincident. Less than 2.7% variation between simulated and analytic results is exhibited for all modulations at $E_b/N_o > 0\ dB$ and $P_b > 10^{-5}$.

B. Multiple Access Performance

Introducing a second network user, the cross correlation over one symbol period between the m^{th} symbol of user v given by (4) and the n^{th} symbol of user w given by (9) can be expressed as given by (10) and (11) [3].

$$s_n^{(w)}(t) = 2\sum_{k=1}^{K} A_k^{(w)} \cos\left[2\pi f_{sb} k t + \phi_k^{(w)} + \theta_n^{(w)}\right] \tag{9}$$

$$R_{mn}^{(vw)} = 2T_{sb}\sum_{k=1}^{K} A_k^{(v)} A_k^{(w)} \cos\left[\Phi_{mn}^{(vw)}(k)\right] \tag{10}$$

$$\Phi_{mn}^{(vw)}(k) = \phi_k^{(v)} - \phi_k^{(w)} + \theta_m^{(v)} - \theta_n^{(w)} - 2\pi f_{sb} k\tau \tag{11}$$

Delay parameter τ in (11) is the relative received time difference between communication symbol boundaries of user v and w. Under synchronized network conditions, ($\tau = 0$) and user symbol boundaries are perfectly aligned during receiver correlation and symbol estimation. For the synchronized MPSK system, assuming 1) data and multiple access phase modulations in (11) are mutually independent $\forall\ m,\ n,\ v$, and w, and 2) data phase modulations (θ) are discrete, uniformly distributed random variables over $[0, 2\pi]$, it can be shown that

$E\left\{R_{mn}^{(vw)}\right\} = 0$ for all M and the variance of (10) can be written as shown in (12) where $F_\phi(j,k)$ equals (13) and (14) for the binary ($M = 2$) and M-ary ($M > 2$) cases, respectively.

$$\text{Var}\left\{R_{mn}^{(vw)}\right\} = 4T_{sb}^2 \sum_{j=1}^{K}\sum_{k=1}^{K} A_j^{(v)} A_j^{(w)} A_k^{(v)} A_k^{(w)} F_\phi(j,k) \tag{12}$$

$$F_\phi^{M=2}(j,k) = \cos\left[\phi_j^{(v)} - \phi_j^{(w)}\right]\cos\left[\phi_k^{(v)} - \phi_k^{(w)}\right] \tag{13}$$

$$F_\phi^{M>2}(j,k) = \cos\left[\phi_j^{(v)} - \phi_j^{(w)} - \phi_k^{(v)} + \phi_k^{(w)}\right] \tag{14}$$

Multiple access interference (MAI) effects are analyzed by introducing an interfering term (N_I) into bit error analysis as an additional noise contribution, e.g., if the MAI can be approximately characterized as relatively wide band then $E_b/(N_o + N_I)$ can replace E_b/N_o in non-network P_b expressions to obtain reasonable approximations. For the spectrally encoded MPSK system under consideration, multiple access interference can be effectively reduced by minimizing (12).

Assuming the multiple access phase modulations (ϕ) in (13) and (14) are uniformly distributed random variables over $[0, 2\pi]$, and equal power is received from all users, it can be shown that the variance expression of (12) identically reduces to the expression in (15) which is valid for all M [3].

$$\text{Var}\left\{R_{mn}^{(vw)}\right\} = 2T_{sb}^2 \sum_{k=1}^{K} A_k^4 \tag{15}$$

In this case, the amount of MAI power ($N_I/2$) impacting detection and estimation is proportional to the variance of $R_{mn}^{(vw)}$ (cross correlation power) [6] and may be expressed as

$$\frac{N_I}{2} \approx \frac{1}{E_S} \sum_{v=1, v\neq w}^{N_U - 2} \text{Var}\left\{R_{mn}^{(vw)}\right\} \tag{16}$$

$$\frac{N_I}{2} \approx \frac{2T_{sb}^2}{E_S}(N_U - 2)\sum_{k=1}^{K} A_k^4 \tag{17}$$

For $M = 2^l$ symbols having $E_s = lE_b$ average energy, the N_I multiple access interference of (17) can be substituted into $E_b/(N_o + N_I)$ as shown in (18) assuming the multiple access interference effects are accurately incorporated as wide band interference. The result of (18) is then substituted into P_b expressions of (7) and (8) as shown in (19) and (20) to obtain analytic MPSK P_b estimates for multiple access networks using $M = 2$ and $M > 2$ communication symbols, respectively.

$$\frac{E_b}{N_o + N_I} = \left[\frac{N_o}{E_b} + \frac{4T_{sb}^2}{l{E_b}^2}(N_U - 2)\sum_{k=1}^{K} A_k^4\right]^{-1} \tag{18}$$

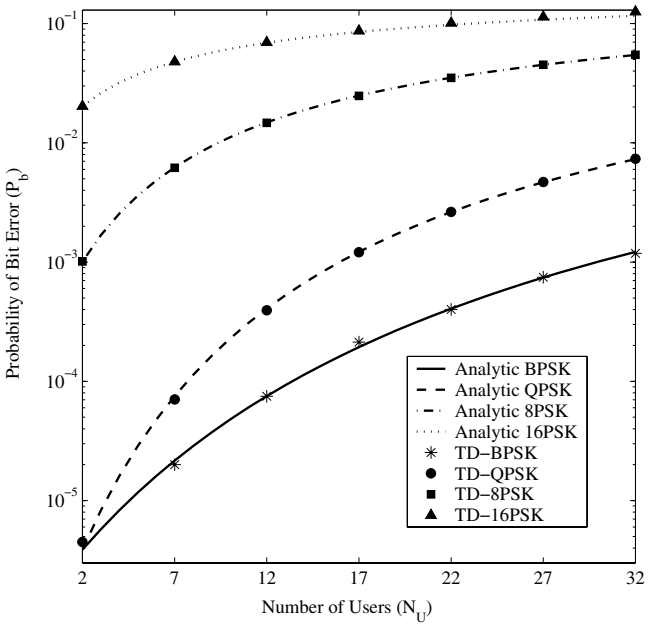

Fig. 2. Multiple Access Communication Performance using Uniformly Distributed Phase Modulation with fixed $E_b/N_o = 10.0\ dB$ (all modulations) and $K = 255$ Sinusoidal Components [3]

$$P_b = Q\left[\sqrt{2\left(\frac{E_b}{N_o + N_I}\right)}\right] \tag{19}$$

$$P_b \approx \frac{2Q}{l}\left[\sqrt{2l\left(\frac{E_b}{N_o + N_I}\right)}\sin\left(\frac{\pi}{M}\right)\right] \tag{20}$$

To verify the theoretical multiple access P_b results presented in (18) through (20), Monte Carlo simulations were conducted using $M = 2,\ 4,\ 8,$ and 16 spectrally encoded MPSK networks containing up to $N_U = 32$ users. For all cases considered, simulated results agreed very favorably with analytic results of (19) and (20) when incorporating multiple access interference according to (18). Representative results of P_b versus N_U for $E_b/N_o = 10.0\ dB$ are shown in Fig. 2. Analysis of data presented in Fig. 2 revealed that simulated and analytic results are nearly identical; approximately 2.5% average error (averaged across N_U) between simulated and analytic results for all modulations and $P_b > 10^{-5}$.

III. Adaptive Interference Avoidance

Adaptive interference avoidance first involves estimating spectral locations where interference is occurring. In Fourier-based spectral estimation, the Discrete Fourier Transform (DFT) can be used as a computational tool to effectively describe the spectral content of a time-sampled electromagnetic environment. Using a given number of equally spaced DFT components, each frequency component is described by frequency, amplitude, and phase parameters [7]. Frequency and

amplitude information can be extracted from the DFT and used to determine which spectral region(s) are clear of interference. The frequency spectrum can be adaptively estimated using any available technique, e.g., periodogram, autoregressive linear predictive filtering, etc, as demonstrated with other interference avoiding transform domain processing techniques [1,2,8].

After normalizing the estimated spectral response, a threshold is established such that all frequency components exceeding the threshold (those containing interference) are assigned a value of zero (0). Frequency components whose magnitudes fall below the threshold are deemed interference free and assigned a value of one (1) [8]; this process yields a vector representing an ideal rectangular spectrum which has been selectively "notched." Assuming the transmitter and receiver observe identical electromagnetic environments, the spectral estimation and thresholding process yields identical "notched" magnitude vectors. An achievable condition assuming all interfering sources are sufficiently removed from the geographical region containing the transmitter and receiver of interest.

Using the "notched" spectrum vector, phase values are assigned to those components which are available for waveform generation, i.e., those with a magnitude of one. This phase coding represents the form of *spectral encoding* employed here and provides the degree of freedom required to enable effective interference avoidance and multiple access capability.

After spectral estimation, thresholding, and spectral encoding, the remaining frequency components are scaled to ensure that equal energy symbols are transmitted, independent of the number of frequency components being used. For example, if only one-third of the available frequency components remain after thresholding, the amount of required energy contained in each remaining component is tripled relative to the case when no interference is present.

IV. Spectral Response and Notching of Narrow Band Interference (NBI)

For demonstrating interference suppression capability, narrow band interference (NBI) is introduced using $P = 31$ sinusoids. Figure 3 shows the spectral response of the NBI considered and the resultant spectral notching mask (dashed line) obtained for a threshold value of 1.0. Equations (21) through (23) analytically describe the NBI where amplitude weights A_p are shown in Fig. 3 and phase values ϕ_p were randomly assigned for each iteration of the simulation.

$$I(f) = \sum_{p=1}^{P} A_p^{(v)} \left[\Delta_p^- + \Delta_p^+\right] \tag{21}$$

$$\Delta_p^- = \delta(f - pf_{sb})e^{+j[\phi_p]} \tag{22}$$

$$\Delta_p^+ = \delta(f + pf_{sb})e^{-j[\phi_p]} \tag{23}$$

For the NBI in Fig. 3, 8 of 31 ($\approx 26\%$) sinusoidal components were notched out using the spectral notching mask

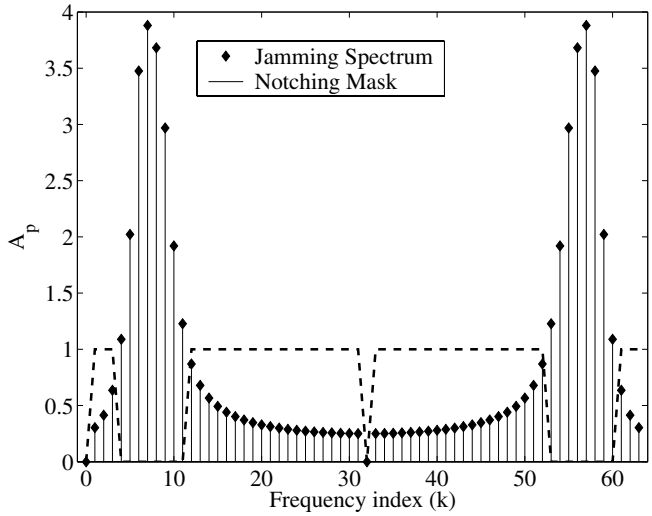

Fig. 3. Spectral Response of Narrow Band Interferer ($P = 31$ Sinusoids) and Spectral Notching Mask (Dashed Line) for Threshold of 1.0

shown. The amplitudes of remaining frequency components were raised by approximately 16% (relative to the non-interferece case) for this 26% NBI case to maintain equal energy conditions. Figure 4 shows NBI effects on MPSK performance for $N_U = 3$ and an interference-to-signal power ratio (I/S) of $3.14\ dB$. Comparison of this data with Fig. 1 clearly shows how the addition of MAI (one additional transmitter) and NBI have severely degraded communication performance.

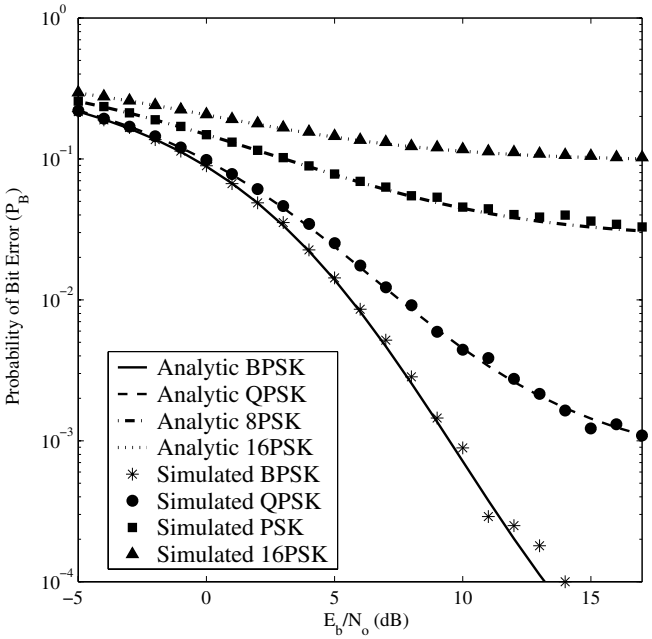

Fig. 4. Narrow Band Interference and $N_U = 3$ Users Present With No Spectral Notching: P_B vs E_b/N_0 for TD-MPSK Signaling with $I/S = 3.14$ dB and $P = 31$ Sinusoids [3]

By way of illustrating the interference avoidance capability of the proposed technique, representative results for QPSK modulation is provided in Fig. 5 for the same I/S of 3.14 dB as used for Fig. 4 data. The significance of each line presented in Fig. 5 is as follows: (1) The unfilled diamond data points represent baseline performance with no multiple access (MAI) or narrow band interference (NBI) present and no spectral components notched, (2) The filled diamond data illustrates performance degradation (relative to the unfilled diamond data) due solely to MAI resulting from one equal power additional user with no NBI present or notching used, (3) The dashed line illustrates performance degradation (relative to the filled diamond data) due to introducing the spectral notch (note that the jammer is *NOT* present in this case and the degradation between the dashed line and filled diamond data is due solely to corruption of communication symbol correlation properties between the two network users even though equal energy signaling is maintained for both); this dashed line represents the best case performance that can be expected when NBI is introduced and notching applied, (4) The filled circle data points represent the case with both MAI and NBI present and no notching applied, and (5) The unfilled circle data represents the case with both MAI and NBI present and spectral notching applied (interference avoidance). The fact that the suppressed data doesn't completely improve to the dashed line is due to NBI energy which remains in spectral components/regions which are outside the notched location(s), i.e., residual NBI energy in sinusoidal components which falls below the threshold and remains after spectral notching. There is approximately 7.5 dB of processing gain (defined here as the reduction in required E_b/N_o to achieve a fixed P_b) achieved at $P_b = 10^{-3}$ when interference avoidance is applied. Similar suppression performance was achieved for all MPSK modulations considered in Fig. 4.

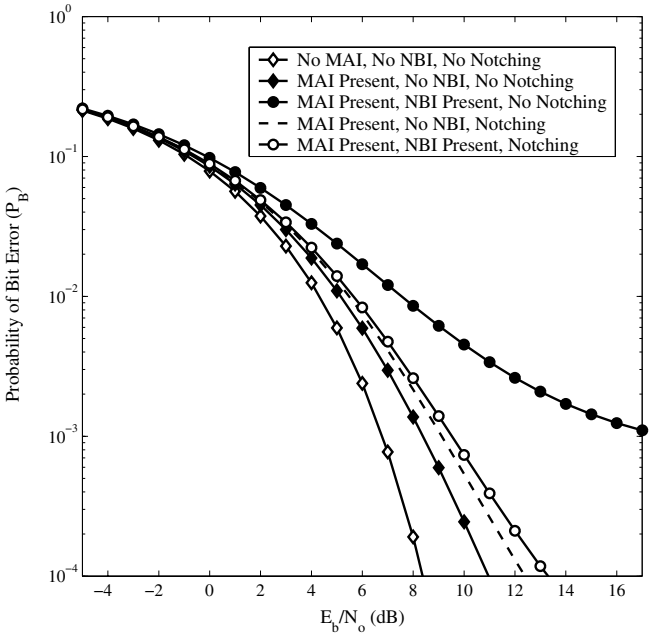

Fig. 5. Illustration of Narrow Band Interference (NBI) Avoidance for QPSK Modulation Using $P = 31$ Sinusoids and $I/S = 3.14\ dB$ [3]

V. Conclusion

Analytic development and simulated multiple access performance results are provided for an interference avoiding, spectrally encoded M-Ary Phase Shift Keyed (MPSK) technique. As developed, the composite phase modulation, consisting of independent data and coded multiple access components, enables effective multiple access capability while spectral estimation and thresholding permits adaptive interference avoidance. In conjunction with providing effective multiple access communications and interference avoidance, the proposed technique is attractive because the phase modulation factors are analytically tractable between frequency and time domains. This permits reliable theoretical performance characterization for variation in multiple access phase modulation assignment. Analytic and simulated results are provided using randomly assigned, uniformly distributed multiple access phase values. Both multiple access communication and narrow band interference avoidance (suppression) are demonstrated. Analytic and simulated P_b versus E_b/N_o performance of a non-network (single channel) spectrally encoded MPSK system is shown consistent with conventional MPSK signaling. For a multiple access network, approximately 2.5% average error between simulated and analytic results is demonstrated in a multiple access environment containing up to 32 users. Up to 7.5 dB of processing gain is demonstrated when interference suppression mechanisms are employed.

References

[1] R. W. Klein, M. A. Temple, R. A. Raines, and R. L. Claypoole, "Interference avoidance communications using wavelet domain transformation techniques," *IEE Electronics Letters*, vol. 37, pp. 987–989, January 2001.

[2] P. J. Swackhammer, M. A. Temple, and R. A. Raines, "Performance simulation of a transform domain communication system for multiple access applications," *Military Communications Conference Proceedings, MILCOM 1999*, vol. 2, pp. 1055–1059, October 1999.

[3] A. S. Nunez, "Interference suppression in multiple access communications using m-ary phase shift keying generated via spectral encoding," Master's thesis, Air Force Institute of Technology, 2004.

[4] R. Van Nee and R. Prasad, *OFDM for Wireless Multimedia Communications*. Boston, Massachusetts: Artech House, 2000.

[5] J. G. Proakis, *Digital Communications*. New York, New York: McGraw-Hill, 4th ed., 2001.

[6] T. Rappaport, *Wireless Communications*. Upper Saddle River, New Jersey: Prentice Hall PTR, 1996.

[7] J. Proakis and D. Manolakis, *Digital Signal Processing, Principles, Algorithms, and Applications*. Saddle River, New Jersey: Prentice-Hall, 1996.

[8] M. Roberts, "Initial acquisition performance of a transform domain communication system: Modeling and simulation results," *MILCOM 2000 Proceedings. 21st Century Military Communications. Architectures and Technologies for Information Superiority*, vol. 2, pp. 1119–1123, 2000.

"The views expressed in this article are those of the author(s) and do not reflect official policy of the United States Air Force, Department of Defense or the U.S. Government."

